

THREE DIMENSIONAL MODELING OF GAS-SOLID COUPLED FREE AND POROUS FLOW IN A FILTRATION PROCESS

Haixia Li *, Bin Li and Xue Bai

School of Mechanical and Power Engineering, Henan Polytechnic University, Jiaozuo 454000, China

Email: lihx@hpu.edu.cn

ABSTRACT

The numerical simulation method is used to analyze the process of particulate removal from high temperature gas by multi-pipe ceramic filters. The gas-solid two-phase flow field in the ceramic filter vessel was simulated using the Eulerian two-fluid model provided by FLUENT code. The ceramic filter vessel contains six ceramic filters, which are arranged in the form of an equilateral hexagon. The variations of pressure distribution in the filter cavity were analyzed and the distribution of dust cake density along the filter length was studied.

Keywords: Numerical simulation, Particulate removal, Ceramic filter, Two-phase flow.

1. INTRODUCTION

Papers should be prepared according to present instructions and printed on high-quality white paper, A4 size. Papers are to be sent to the Editor or the managing editor who handled your manuscript.

Manuscripts not complying with present instructions may not be published. The ceramic filter has been considered to be one of the most promising technologies for particle separation from gas at high temperatures, owing to its high filtration efficiency, heat-shock resistance, and gas erosion resistance [1,2]. There are many problems that threaten the stability and reliability of the filtration process [3-4], such as the bridging of dust cakes between adjacent filters, due to uneven particle removal [5]. Uneven particle removal leads to a gradual increase of local particle layer thickness. This causes a particle bridge to occur, which then damages the filters [6,7]. Groups of candle filters are periodically cleaned by a rapid back pulse of compressed air to remove the dust cake that builds up on filter surfaces and to regain filtration pressure [3]. The efficiency of the back pulse is an important factor for long term, steady operation. It is therefore important to analyze unsteady gas and particle flow during back pulse cleaning, in order to understand the mechanism of back pulse and optimization of the filter vessel structure [4]. Recent research on the back pulse process in ceramic filters has focused on the gas flow field [8,9] and dust cake structure [10-13]. Particle movement during the back pulse process has not been studied in the literature.

The aim of the present work is to obtain a relative numerical model and use this model to study the filtration and back pulse process in a ceramic filter. The gas and particle flow both during and after the reverse pulse flow process is described. The particle concentration distribution along the filter surface is also studied.

2. MODELS AND BOUNDARY CONDITIONS

2.1. Simulation mode

The filter vessel models the particulate removal system for the coal gasification process and accommodates six ceramic filters, which are arranged in a regular hexagon. The type of ceramic filter used in the present model is a DIA-SCHUMALIT®H 10-20. The inside and outside diameter are 4 and 6cm, respectively, and the filter length is 1.5m. The aperture of porous film on the filter body is about 10-15 μ m. The straight nozzle, whose inner diameter is 6mm, is located above the diffuser. The gap between the nozzle tip and the diffuser top is 50mm. A schematic diagram of the filter vessel geometry and the measurement points is shown in Figure 1. The raw gas inlet is located at one side of the filter vessel; positioned 200mm under the bottom of the filter element (the closed end of the filter element). The origin of the coordinate system is set at the center of the section that is on the same horizontal axis as the bottom of the filter element. The z-axis (the longitude coordination), starting from the closed end of the filter element, is contrary to gravitational direction. In order to identify the relative position of the filters, the six filters are named, in counterclockwise sequence, f1, f2, f3, f4, f5, and f6.

The Reynolds stress transport model accounts for the evolutions of the individual stress components, and thus completely avoids the use of an eddy viscosity. It is also well suited for handling anisotropic turbulence fluctuations. Therefore, in this study, it is applied to simulate gas flow, in view of the flow condition during the filtration and pulse cleaning process, where only two candle filters out of six are to be cleaned. In the Eulerian approach, the two phases are considered to be separate interpenetrating continua and separate (but coupled) equations of motion, with separate

boundary conditions solved for each phase. Conservation equations for each phase are derived to obtain a set of equations, which have a similar structure for all phases.

The operation parameters are selected from an industry design of a ceramic filtration system. The filtration velocities are 1, 2 and 3cm/s, with the operating pressure being 4.0 MPa and the temperature being 673 K. The particle load is 10g/Nm³. The densities of gas and particles in this model are 22.4 and 2000kg.m⁻³, respectively. The mean particle diameter is 3µm.

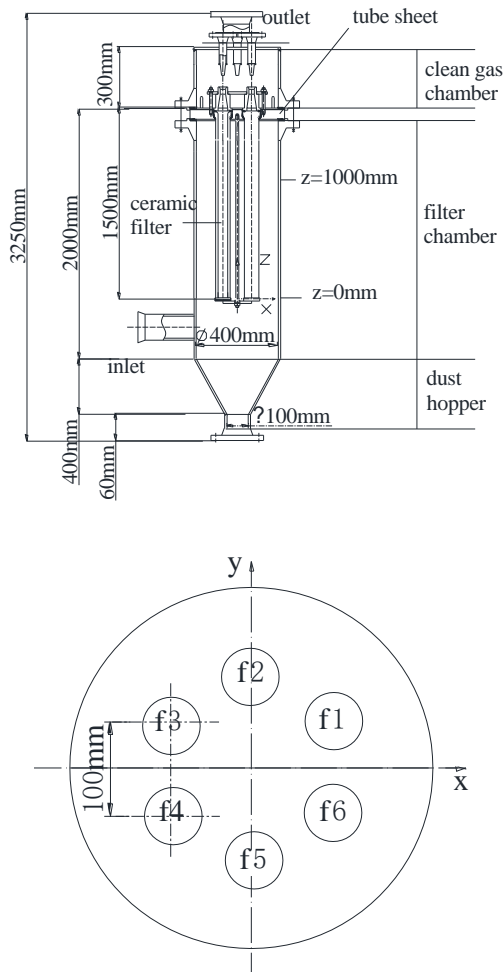


Figure 1. Schematic diagram of the filter vessel

2.2. Grid partition

Considering the large outline and complex configuration of the filter vessel, a blend of structure and non-structure grids are used to simulate flow field. The grid cells used in the work is shown in Figure 2. In order to get an appropriate solution, independent of grid, different grids are used to simulate filtration gas flow in the filter vessel. Patankarhe gave a method of resistance distribution, namely the porous medium model, to simulate flow field in a porous material. This method considers the effect of solid structure on the fluid flow to be resistance acting on a fluid. So, fluid flow in a porous medium can be simulated with a coarse grid [14].

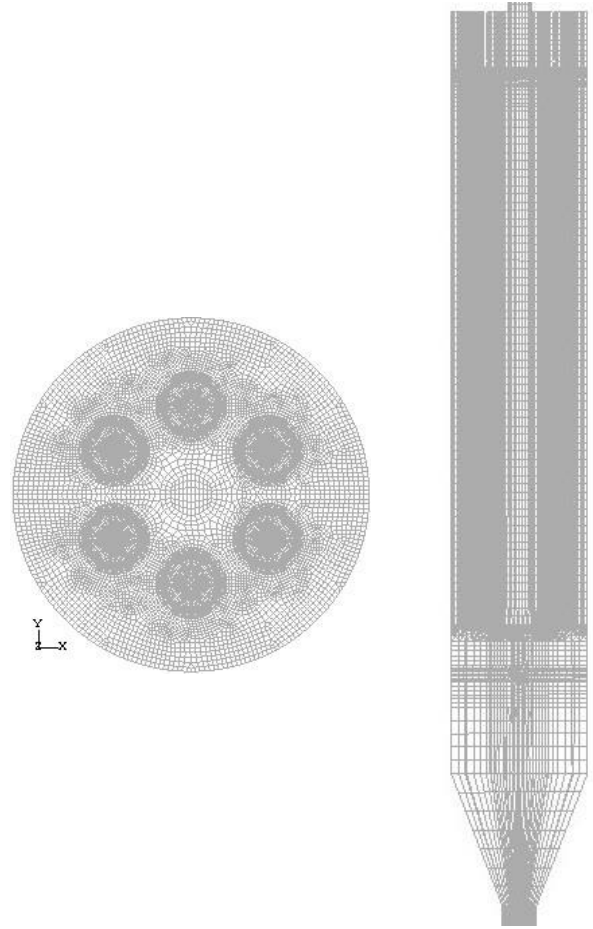


Figure 2. Schematic diagram of grids of filter vessel

2.3. Boundary conditions

The velocity inlet boundary condition is used. Gas and particulates are fully mixed, before they enter the filter vessel at a constant velocity of 7.5 m.s⁻¹.

2.4. Porous media model

Porous media are modeled by the addition of a momentum source term to the standard fluid flow equations. The source term is composed of two parts: a viscous loss term (the first term on the right-hand side of Equation (1)); and an inertial loss term (the second term on the right-hand side of Equation (1)). The porous material affects the flow dynamics through the momentum equation. This contributes to the pressure gradient in the porous cell, creating a pressure drop that is proportional to the fluid velocity (or velocity squared) in the cell.

$$\Delta p = -\frac{\mu}{\alpha} l v - \frac{1}{2} c_2 \rho l |v| v \quad (1)$$

In laminar flows through porous media, the pressure drop is typically proportional to velocity and the constant C_2 can be considered to be zero. Ignoring convective acceleration and diffusion, the porous media model then reduces to Darcy's Law:

$$\Delta p = -\frac{\mu}{\alpha} l v \quad (2)$$

The ceramic filters are treated as porous media with a given permeability. The penetration of gas through the porous filter wall is then computed using Darcy's Law as part of the solution.

Here, Δp is seepage pressure drop, μ is gas molecular viscosity, which is a function of temperature, α is permeability, which is $1 \times 10^{-12} \text{ m}^2$ for the porous wall of the ceramic filter in this simulation, v is gas filtration velocity, l is the porous medium thickness, C_2 is the inertial resistance factor, and ρ is density.

The pressure drop of gas flow through filter cake can be estimated using the Ergun Equation [15], which is shown as the following equation (3).

The Ergun Equation is used to derive porous media inputs for a packed filter cake. In turbulent flows, packed filtration cakes are modeled using both a permeability and an inertial loss coefficient. One technique for deriving the appropriate constants involves the use of the Ergun equation, which is a semi-empirical correlation applicable over a wide range of Reynolds numbers and for many types of packing:

$$\frac{\Delta p}{l} = \frac{150\mu(1-\varepsilon)^2}{d_p^2\varepsilon^3} v + \frac{1.75\rho(1-\varepsilon)}{d_p\varepsilon^3} v^2 \quad (3)$$

When modeling laminar flow through a packed filtration cake, the second term in the above equation may be ignored, resulting in the Blake-Kozeny equation [15].

$$\frac{\Delta p}{l} = \frac{150\mu(1-\varepsilon)^2}{d_p^2\varepsilon^3} v \quad (4)$$

In these equations, d_p is the mean particle diameter, l is the cake thickness, and ε is the void fraction; defined as the volume of voids divided by the volume of the packed filtration cake region. Comparing equation (1) with (3), the permeability and inertial loss coefficient in each component direction may be identified as:

$$\alpha = \frac{d_p^2\varepsilon^3}{150(1-\varepsilon)^2} \quad (5)$$

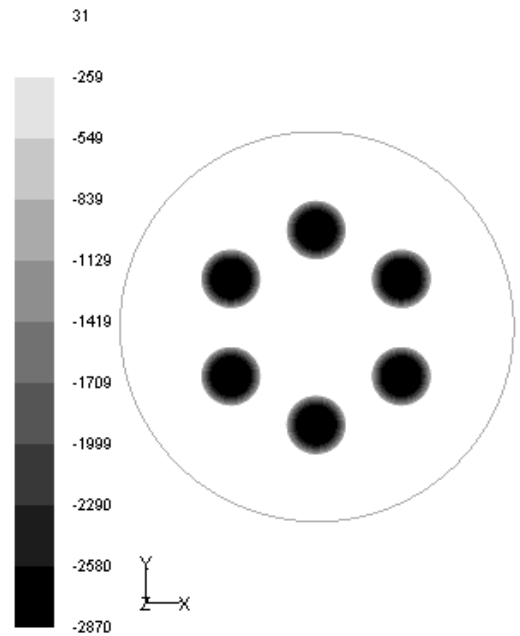
$$c_2 = \frac{3.5(1-\varepsilon)}{d_p\varepsilon^3} \quad (6)$$

A pressure drop will also occur when gas penetrates through the dust cake. Both the local thickness (l) of the dust cake on the outside of the filter surface and the permeability (α) will change with the deposition of particles on the filter surface during the filtration process in this simulation. This is because the permeability near ceramic filters will vary when more dust is deposited on the filter surface. The effect of the filter cake on the flow condition is added to the model by a user-defined function, which describes the variation of pressure difference with the change of filter cake density.

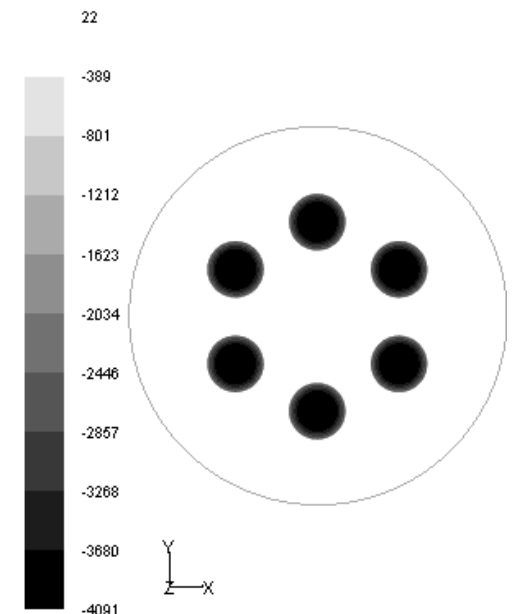
3. RESULTS AND DISCUSSION

Figure 3 shows pressure distribution during the filtration and pulse cleaning process in the plane of $z=1\text{m}$, when filtration velocity is 2cm/s . It can be seen that the pressure

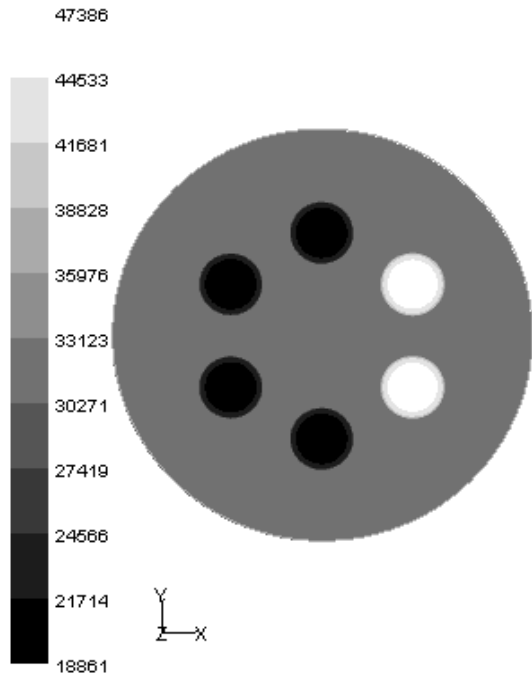
outside the candle filter is higher than that inside the candle filter during the filtration process. The pressure decreases gradually from filter chamber to filter cavity. The pressure drop occurs mainly due to the filter porous wall, through which gas enters the filter cavity and on which particles are intercepted. Figures 3 (a) and (b) show that the pressure difference across the filter wall increases with filtration time. This is because more particulates will settle on the filter surface as the filtration process is carried out, resulting in greater flow resistance. The pressure will increase rapidly in the filter cavity of the filter undergoing pulse cleaning, which is shown in Figure 3(c). The pressure inside the filter undergoing cleaning is higher than that in the filter chamber, so a reverse force can flow the particulates from the filter surface. The pulse duration is one second. The pressure inside the filter undergoing pulse cleaning will decrease gradually back to normal filtration conditions after the pulse cleaning process, as shown in Figure 3(d).



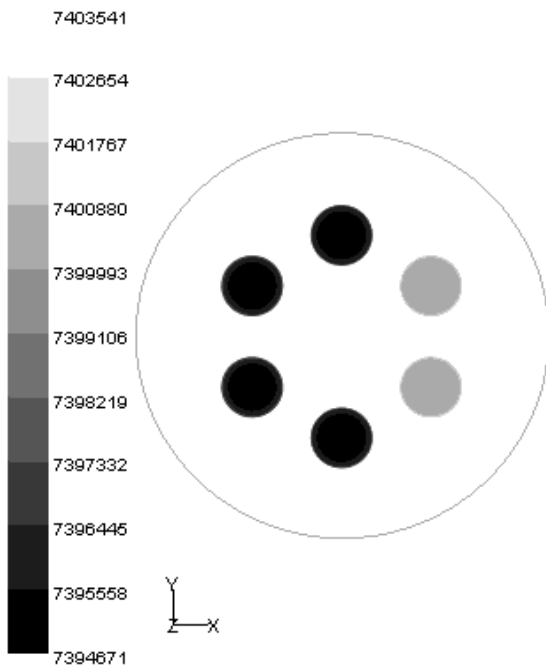
(a) Filtration time is 200s



(b) Filtration time is 300s



(c) 0.1 s after the beginning of pulse cleaning



(d) 120s after pulse cleaning

Figure 3. Pressure distribution in the plane $z=1m$ during filtration and pulse cleaning process (the value unit in this figure is Pa)

Figure 4 shows the variation of dust cake area density along the candle filter length. The particle concentration near the filter surface is lower at both ends of the candle filter than at the middle position. Particle concentration increases along the

axial direction in the middle of the candle filter. Dust cake area density increases when filtration velocity increases, because more particles will be deposited on the filter surface, compared with the same particle concentration of inlet flow at the same time.

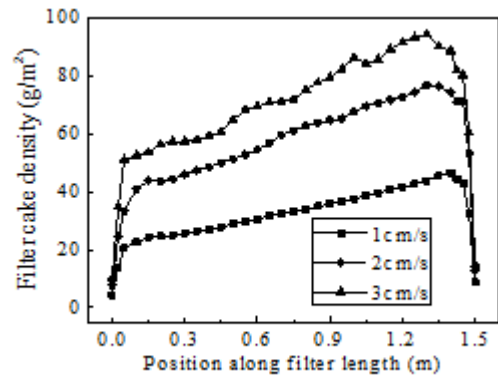


Figure 4. Variation of dust cake area density along an axial direction at different filtration velocities

Figure 5 shows the variation of pressure drop across the filter in an axial direction. The resistance of gas flow penetrating the porous wall enhances when filtration velocity increases. The higher filtration velocity will lead to more particles settling on the filter surface, and then greater flow resistance will occur, when gas goes through the porous filter wall. Pressure drop therefore increases with filtration velocity increase.

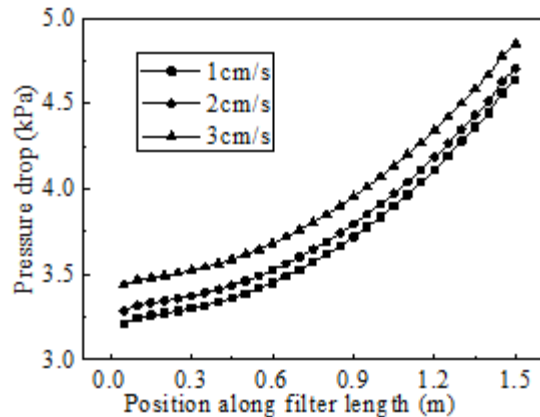


Figure 5. Distribution of pressure drop across a porous wall along axial an direction at different filtration velocities

Figure 6 shows filter cake area density distribution along an axial direction for different dust loads of inlet flow. The cake density increases from the closed end to the upper opening of the candle filter and decreases near the vicinity of the tube sheet. The distribution patterns of filter cake density are identical for different particle load inlet flows. The filter cake area density increases with particle load increase, as more particles will be deposited on the filter surface.

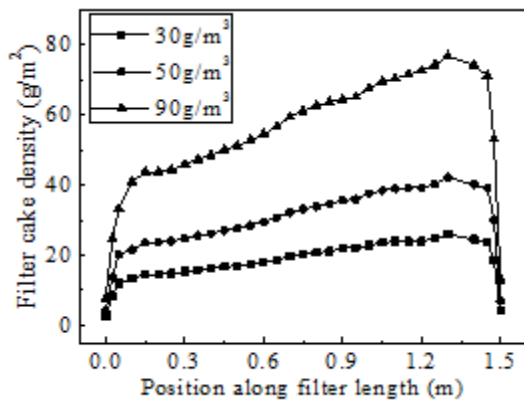


Figure 6. Variation of filter cake area density along an axial direction for different particle load

Figure 7 shows the variation of pressure drop across the filter porous wall along the filter length when dust loads of inlet gas flow are 30, 50 and 90 g/m³. It can be seen that pressure drop across the filter wall increases from the closed end to the open end of the candle filter. More particles will settle on the outer surface when the particle concentration in the inlet flow increases. Higher pressure drop across the filter wall will therefore occur with a particle load increase, within the same filtration time.

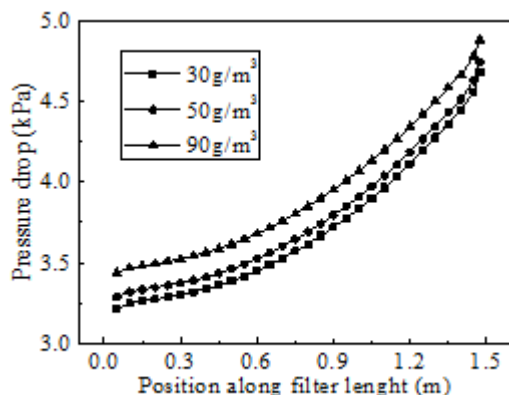


Figure 7. Pressure drop distribution along the axial direction for different particle loads

4. CONCLUSIONS

In this work, a computer simulation procedure for analyzing gas-particle flow during the pulse cleaning process in a filter vessel containing six ceramic filters is described. Pressure drop in the filtration system mainly occurs in the porous wall and dust cake. Pressure drop increases in the axial direction along the filter length. More energy is therefore needed when clearing the dust cake. The dust cake area density is relatively higher at the middle position of the candle filter than near the two ends of the candle filter. The results show that filtration velocity has a great effect on the formation of the dust cake. Both pressure drop and dust cake area density increase with filtration velocity.

ACKNOWLEDGMENT

The author acknowledges the funding support of the national natural science foundation of china (No.U1504217),

the Key Subject of Henan Province (No.507908), the Key Scientific and Technological Project of Henan Province (No.102102210209) and Natural Science Program of Henan Province (No.2010B470005) for this research.

REFERENCES

1. S. Callw, P. Contal, D. Thomas, D. Bemer, "Description of the clogging and cleaning cycles of filter media," *Powder Technology*, Vol.123, pp. 40-52, 2002. DOI: [10.1016/S0032-5910\(01\)00430-2](https://doi.org/10.1016/S0032-5910(01)00430-2).
2. Z.L. Ji, M.X. Shi, F.X. Ding, "Transient flow analysis of pulse-jet cleaning system in ceramic filter," *Powder Technology*, Vol.139, pp. 200-207, 2004. DOI: [10.1016/j.powtec.2003.11.004](https://doi.org/10.1016/j.powtec.2003.11.004).
3. H.X. Li, Z.L. Ji, X.L. Wu, J.H. Choi, "Numerical analysis of flow field in the hot gas filter vessel during the pulse cleaning process," *Powder Technology*, Vol.173, pp.82-92, 2007. DOI: [10.1016/j.powtec.2006.10.042](https://doi.org/10.1016/j.powtec.2006.10.042).
4. Z.L. Ji, S.Peng, H.H. Chen, M.X. Shi, "Numerical calculation of transient flow field of ceramic candle filter during pulse cleaning process," *Journal of Chemical Engineering*, Vol.54, pp.35-41, 2003.
5. J.F. Qiu, T.X. Xu, L.T. Zhang, J. Hui, "Transient flow model solution of reverse jet pulse cleaning system in high temperature ceramic filter," *Journal of Xian Jiaotong University*, Vol.38, pp. 15-18, 2004.
6. H.Q. Jiao, Z.L. Ji, H.H. Chen, M.X. Shi, "Influence of operating parameters on pulse cleaning process of ceramic filter," *Journal of Chemical Engineering*, Vol.55, pp. 1156-1161, 2004.
7. D.Koch, J.Swille, R.Clift, "Dust cake detachment from gas filter," *Powder Technology*, Vol.86, pp. 21-29, 1996. DOI: [10.1016/0032-5910\(95\)03033-6](https://doi.org/10.1016/0032-5910(95)03033-6).
8. A. Goodarz, H.S. Duane, "Analysis of steady-state filtration and back pulse process in a hot-gas filter vessel," *Aerosol Science Technology*, Vol. 36, pp. 665-677, 2002. DOI: [10.1080/02786820290038357](https://doi.org/10.1080/02786820290038357).
9. T. Katsuka, H. Satone, T. Yamada, T. Mori, J. Tsubaki, "Development of a novel high performance filtration system—Optimization of operating conditions," *Powder Technology*, Vol.207, pp. 154-158, 2011. DOI: [10.1016/j.powtec.2010.10.022](https://doi.org/10.1016/j.powtec.2010.10.022).
10. Z.L. Ji, H.Q. Jiao, H.H. Chen, "Image analysis on detachment process of dust cake on ceramic candle filter," *Chinese Journal of Chemical Engineering*, Vol.13, pp.178-183, 2005.
11. H.C. Chi, Z.L. Ji, D.M. Sun, L.S. Cui, "Experimental investigation of dust deposit within ceramic filter medium during filtration-cleaning cycles," *Chinese Journal of Chemical Engineering*, Vol.17, pp. 219-225, 2009. DOI: [10.1016/S1004-9541\(08\)60197-4](https://doi.org/10.1016/S1004-9541(08)60197-4).
12. Z.L. Ji, H.X. Li, X.L. Wu, J.H. Choi, "Numerical simulation of gas/solid two-phase flow in ceramic filter vessel," *Powder Technology*, Vol. 1, pp. 91-96, 2008. DOI: [10.1016/j.powtec.2007.03.009](https://doi.org/10.1016/j.powtec.2007.03.009).
13. T. Deuschle, U. Janoske, M. Piesche, "A CFD-model describing filtration, regeneration and deposit rearrangement effects in gas filter systems," *Chemical Engineering*, Vol.135, pp. 49-55, 2008. DOI: [10.1016/j.cej.2007.03.019](https://doi.org/10.1016/j.cej.2007.03.019).

14. X. Zhang, H. Li, C. Yao, "Compressible gas flow in porous media/fluid coupled areas," *Journal of Chemical Engineering*, Vol. 24, pp. 1209-1214, 2003.

15. S. Ergun, "Fluid flow through packed columns," *Chemical Engineering Progress*, Vol.48, pp.89-94, 1952.